Synthesis and Characterization of Graphene/ Molybdenum Disulfide (MoS2) Polymer Nanoparticles for Enhanced Photothermal Cancer Therapy

Mourtas Spyridon [1,2] *

Abstract

Background: Nanoparticle-based therapies have revolutionized cancer treatment, with photothermal therapy (PTT) emerging as a promising approach due to its targeted and minimally invasive nature. Combining PTT with functionalized nanomaterials enhances precision and reduces toxicity, making it a focal point of advanced cancer therapeutics. This study aimed to develop and evaluate graphene and molybdenum disulfide (MoS2) functionalized with copolymers to enhance their biocompatibility and photothermal efficacy in cancer treatment. **Methods:** Graphene and MoS2 were functionalized using diblock copolymers and a statistical copolymer composed of 2-(dimethylamino)ethyl methacrylate (DMAEMA) and benzyl methacrylate (BzMA). The diblock copolymers' monomer composition was varied to study behavior at pH 6, 7, and 8. Exfoliation techniques were optimized for single-layer structures, confirmed via UV-Vis spectroscopy. Dynamic Light Scattering (DLS) was used to assess nanoparticle size and micelle formation. Photothermal performance of the functionalized nanomaterials was evaluated under light irradiation. **Results:** UV-Vis spectroscopy confirmed successful exfoliation of monolayer graphene and MoS2, with notable absorption peaks indicative of their structural integrity. Dynamic Light Scattering showed consistent micelle formation, with nanoparticle sizes optimized for cellular uptake. Functionalized MoS2 demonstrated superior photothermal conversion efficiency, achieving significant localized heat generation under near-infrared light, compared to graphene. Both materials exhibited stability and biocompatibility at physiological and acidic pH levels, critical for cancer environments. **Conclusion:** Functionalized graphene and MoS2 show promise as photothermal agents, offering efficient, targeted cancer cell ablation while minimizing damage to healthy tissues. These findings underscore the potential of combining advanced nanomaterials with PTT for enhanced cancer therapy.

Keywords: Photothermal therapy, Graphene, Molybdenum disulfide, Nanoparticle functionalization, Cancer treatment

Significance | Graphene and MoS2 functionalized with copolymers offer enhanced biocompatibility and efficiency for targeted cancer treatment via photothermal therapy.

*Correspondence. Mohammad Esmaeil Hejazi, MD, Tuberculosis and Lung Diseases, Research Center, Tabriz University of medical science, Tabriz, Iran
E-mail: mehjz@yahoo.com

Editor Md. Shariful Islam, Ph.D., And accepted by the Editorial Board September 17, 2024 (received for review July 23, 2024)

Introduction

Nanotechnology has revolutionized the field of cancer therapy, particularly through the development of innovative nanomaterials for targeted drug delivery systems. Among the various approaches, photothermal therapy (PTT) has gained substantial attention due to its ability to selectively ablate cancer cells by generating localized heat upon exposure to light, typically in the near-infrared (NIR) region. This method minimizes the impact on healthy cells and offers a promising alternative to conventional cancer treatments, such as chemotherapy and radiation therapy, which often come

Author Affiliation.
[1] Dep. Chem. UPAT, University of Patras University of Patras, Greece.
[2] Laboratory of Pharmaceutical Technology, Dept. of Pharmacy, School of Health Sciences, University of Patras, 26510 Rio, Greece.

Please Cite This:
Mourtas Spyridon (2024). "Synthesis and Characterization of Graphene/Molybdenum Disulfide (MoS2) Polymer Nanoparticles for Enhanced Photothermal Cancer Therapy", Biosensors and Nanotheranostics, 3(1),1-12,9899

with significant side effects (Chen et al., 2018). In recent years, two-dimensional (2D) materials such as graphene and molybdenum disulfide (MoS_2) have emerged as potential candidates for PTT due to their unique physicochemical properties, including strong optical absorption, high surface area, and excellent thermal conductivity (Dong et al., 2017).

Graphene, a single layer of carbon atoms arranged in a hexagonal lattice, has been extensively studied for its applications in biomedicine due to its exceptional thermal and electrical conductivity, mechanical strength, and ease of functionalization. In the context of cancer therapy, graphene-based nanomaterials have demonstrated efficient photothermal conversion, making them ideal candidates for PTT (Geim & Novoselov, 2017). By functionalizing graphene with biocompatible polymers, its stability and dispersibility in aqueous environments can be enhanced, reducing potential toxicity and improving its ability to target cancer cells. Furthermore, the conjugation of graphene with polymers allows for the incorporation of other therapeutic agents, enabling the development of multifunctional platforms for synergistic cancer treatment.

Molybdenum disulfide (MoS_2), another promising 2D material, has recently garnered attention for its potential applications in PTT. MoS_2 exhibits strong absorption in the NIR region, making it a highly efficient photothermal agent. Additionally, MoS_2 possesses semiconductor properties that are advantageous for various biomedical applications, including imaging and drug delivery (Hong et al., 2020). Similar to graphene, MoS_2 can be functionalized with polymers to improve its stability and biocompatibility in physiological environments. The exfoliation of MoS_2 into monolayers is particularly important, as monolayer MoS_2 exhibits enhanced optical properties compared to its bulk counterpart, thereby improving its photothermal conversion efficiency.

In this study, both graphene and MoS_2 were functionalized with diblock copolymers and statistical copolymers composed of 2-(dimethylamino)ethyl methacrylate (DMAEMA) and benzyl methacrylate (BzMA). The aim of this work is to investigate the effects of polymer composition and pH on the exfoliation and photothermal properties of graphene and MoS_2 nanoparticles. By varying the weight percentages of DMAEMA and BzMA, the hydrodynamic diameters, micelle formation, and photothermal conversion efficiency of the resulting nanoparticles were systematically studied. The diblock copolymers used in this study were labeled RT-P7, RT-P8, and RT-P9, corresponding to different ratios of DMAEMA-BzMA, while a statistical copolymer (RT-P10) was used as a control. These polymers were selected for their ability to form micelles in aqueous solutions, which can enhance the dispersion and stabilization of the nanoparticles (Dong et al., 2017).

The fabrication of the graphene and MoS_2 nanoparticles was achieved through liquid exfoliation, a method that utilizes ultrasonication to disperse 2D materials in solution. Exfoliation was carried out at three different pH levels (6, 7, and 8) to examine the influence of protonation and deprotonation on the stability and photothermal properties of the nanoparticles. UV-Vis spectroscopy was employed to characterize the optical absorption properties of the exfoliated graphene and MoS_2, particularly in the NIR region, where photothermal conversion occurs (Dreyer et al., 2016). Dynamic light scattering (DLS) was used to measure the hydrodynamic diameters of the nanoparticles, providing insight into their size and potential for micelle formation in aqueous environments.

The photothermal properties of the exfoliated nanoparticles were evaluated through photothermal tests under NIR laser irradiation. This analysis was crucial in determining the efficiency of the nanoparticles in converting light energy into heat, a key factor in the success of PTT. By comparing the photothermal performance of graphene and MoS_2 functionalized with different diblock and statistical copolymers, this study aims to identify optimal conditions for the fabrication of nanoparticles with enhanced photothermal efficiency for cancer treatment (Chen et al., 2018).

The objective of this research is to develop a novel nanomaterial-based platform for PTT using functionalized graphene and MoS_2 nanoparticles. By investigating the effects of polymer composition and pH on the exfoliation and photothermal properties of these nanoparticles, this study seeks to contribute to the advancement of targeted cancer therapies. The results of this work may have significant implications for the development of biocompatible, high-performance photothermal agents that can be used in clinical applications for cancer treatment.

2. Materials and Methods

The polymers used in this project were being prepared beforehand, whereby all of the diblock and statistical copolymers consist of 2-(dimethylamino)ethyl methacrylate (DMAEMA) and benzyl methacrylate (BzMA). The polymers handed were labelled with RT-P7, RT-P8 and RT-P9, which are represented by D7, D8 and D9 respectively with MW of 9000 g mol-1 and weight percentages (wt%) of DMAEMA-BzMA of 90-10, 80-20 and 70-30 respectively. On the other hand, statistical copolymer that was labelled with RT-P10 and represented by D10 have MW of 7000 g mol-1 with weight percentage (wt%) of DMAEMA-BzMA of 80-20. The graphite powder (<150 μm, 99.99% trace metal basis) was purchased from Aldrich, United Kingdom (UK) and molybdenum(IV) disulfide (MoS2) powder (metals basis) was purchased from Alfa Aesar, United Kingdom (UK).

2.1 Fabrication of Nanoparticles

All the diblock and statistical copolymers incorporated with either graphene or MoS2 were being fabricated via exfoliation at three different pH which are pH 6, pH 7 and pH 8. Initially solutions of

pH 5 and pH 9 were prepared, in which the error of buffering ability of the polymer will be further discussed in results and discussions section. Thus, pH 5 solutions were prepared by preparing 1M of Hydrochloric acid (HCl) which was purchased from VWR Chemicals, United Kingdom (UK) and were diluted into distilled water until the pH reached pH 5, which was confirmed by using litmus paper that was purchased from VWR Chemicals, United Kingdom (UK) and pH meter purchased from Hanna Instruments, United States. Meanwhile pH 9 solutions were prepared by preparing 1M of Sodium Hydroxide (NaOH) which was purchased from VWR Chemicals, United Kingdom (UK) and were diluted into distilled water until it reached pH 9, and was confirmed by using litmus paper that was purchased from VWR Chemicals, United Kingdom (UK) and pH meter purchased from Hanna Instruments, United States.

2.1.1 Exfoliation of Nanoparticles

All the diblock and statistical nanoparticles solutions were prepared by following ratio of 1 mg/ mL-1 of copolymer to 0.5 mg/ mL-1 of graphene/MoS2. Thus each of the diblock and statistical copolymer samples were weighed between 5mg to 12.5mg into individual glass vials. Then the graphene/MoS2 powder were weighed separately according to the ratio stated above, and it was then subsequently being added into the vials containing polymers respectively. Distilled water was then being added with respect to the volume amount of graphene/MoS2 in the vials, and all the prepared solutions were then

being subjected to the liquid exfoliation method. The exfoliation of all the diblock and statistical nanoparticles solutions was done firstly in sonic bath (ultrasonic cleaner, USC - TH) purchased from VWR, United Kingdom (UK) for 2 hours. Then the solutions were washed via centrifugation at 700 rpm, 1000 rpm, 1500 rpm, 2000 rpm and 2500 rpm by using Sorvall Lynx 6000 Centrifuge, Thermo Fisher Scientific for 30 minutes each speed. UV-Vis were done in between the centrifuge speed. The same solutions preparation and exfoliation steps were done for pH 6 (HCl) and pH 8 (NaOH) but with the centrifuge speeds of 700 rpm, 1000 rpm, 1500 rpm, 2000 rpm, 2500 rpm, 3000 rpm, 4000 rpm and 5000 rpm.

Partly due the separation between particles in the suspension, in which the sedimentation phenomena that allows the particles to settle at the bottom of a vessel due to the presence of gravity, thus rotation speeds of the centrifuge speeds in this project will be presented in G-force where the speeds in revolutions per minute (rpm) mentioned above are converted into G-force with unit of relative centrifugal force (rcf) by using the Equation 1 as follow :-

G-force (rcf) = $1.12 \times R \times (rpm/1000)2$……..Equation 2.1

where:

R is the radius of rotation of 106 mm in which can be measured at the bottom of the tube (Rmax).

2.2.2 UV-Vis Spectroscopy Ultraviolet-Visible (UV-Vis)

Spectroscopy was done by using Perkin Elmer Lambda 25 UV-Vis Spectrometer in between every centrifuge speed. UV-Vis spectroscopy was carried out to determine the absorbance spectra of all the diblock and statistical copolymer incorporated with either graphene or MoS2 in the near-infrared (NIR) region. UV-Vis spectrum was collected between 300 - 1000nm wavelength, with scan speed of 480nm/min and data interval of 1.

2.3 Characterisation of Nanoparticles

2.3.1 Characterisation in Organic Solvents

The Molar Mass (MM), Molar Mass Distribution (MMD), chemical structure and composition of all the diblock and statistical copolymers were determined in organic solvents. The MM and MMD were obtained via GPC, meanwhile the chemical structure and composition were obtained via 1H NMR. Prior to both analysis, all the samples were prepared to total concentration of 25 mg/mL-1 in which each diblock and statistical copolymers was sonicated in Tetrahydrofuran (THF) for 2 hours and 6 hours separately and subsequently been centrifuged at 700 rpm.

2.3.1.1 Gel Permeation Chromatography (GPC)

Gel Permeation Chromatography (GPC) characterisation was done by using an Agilent, SECcurity GPC system, with a Polymer Standard Service (PSS) SDV analytical linear M column (SDA083005LIM). The mobile phase containing THF of 5 volume % triethylamine was pumped using a "1260 Iso" isocratic pump with a flow rate at 1 mL min-1. This characterization was used to analyse the MW and MWD of all the diblock and statistical copolymers. Prior to GPC analysis, all the samples need to be filtered through Millex-LCR, non-sterile, HPLC certified, syringe-driven filters, which were purchased from Milipore. The analysis started off with measuring refractive index (RI) signal by using an Agilent 1260 RI detector. Simultaneously, the MW and MWD of all the diblock and statistical copolymers used were obtained and recorded based on the calibration curve of six narrow MW linear poly(methyl methacrylate)s (PMMAs) standard samples (2000, 4000, 8000, 20000, 50000 and 100000 g mol-1), which were purchased from Fluka, Aldrich, UK.

2.3.1.2 Proton Nuclear Magnetic Resonance Spectroscopy (1H-NMR)

Proton Nuclear Magnetic Resonance Spectroscopy (1H NMR) spectra of all the diblock and statistical copolymers were obtained by using a 400-MHz Avance Bruker NMR Spectrometer instrument with deuterated chloroform, CDCl3 used as the NMR solvent. 1H NMR spectroscopy was used to analyse the chemical structure and composition of all the diblock and statistical copolymers.

2.3.2 Characterisation in Aqueous Solutions

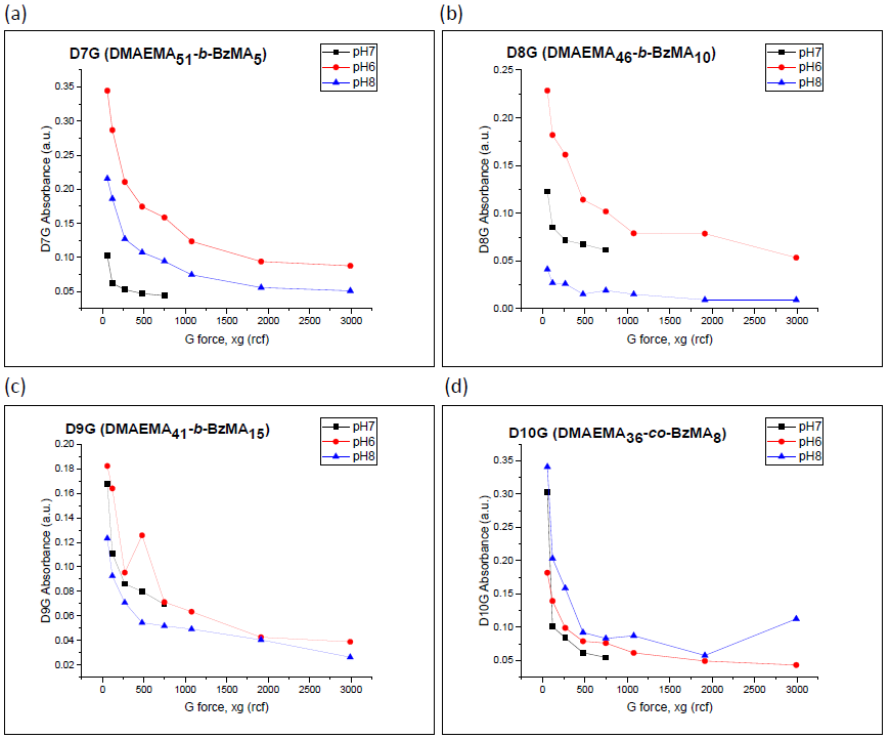

Figure 1. UV-Vis-NIR absorbance spectras of DMAEMA – BzMA of the diblock copolymers, a) D7G, b) D8G, c) D9G and the statistical copolymer, d) D10G. Each is exfoliated with graphene at pH6, pH7 and pH8 and coloured in red, black and blue, respectively. The graphs show the absorbance intensity as a function of centrifugation velocity in g-force.

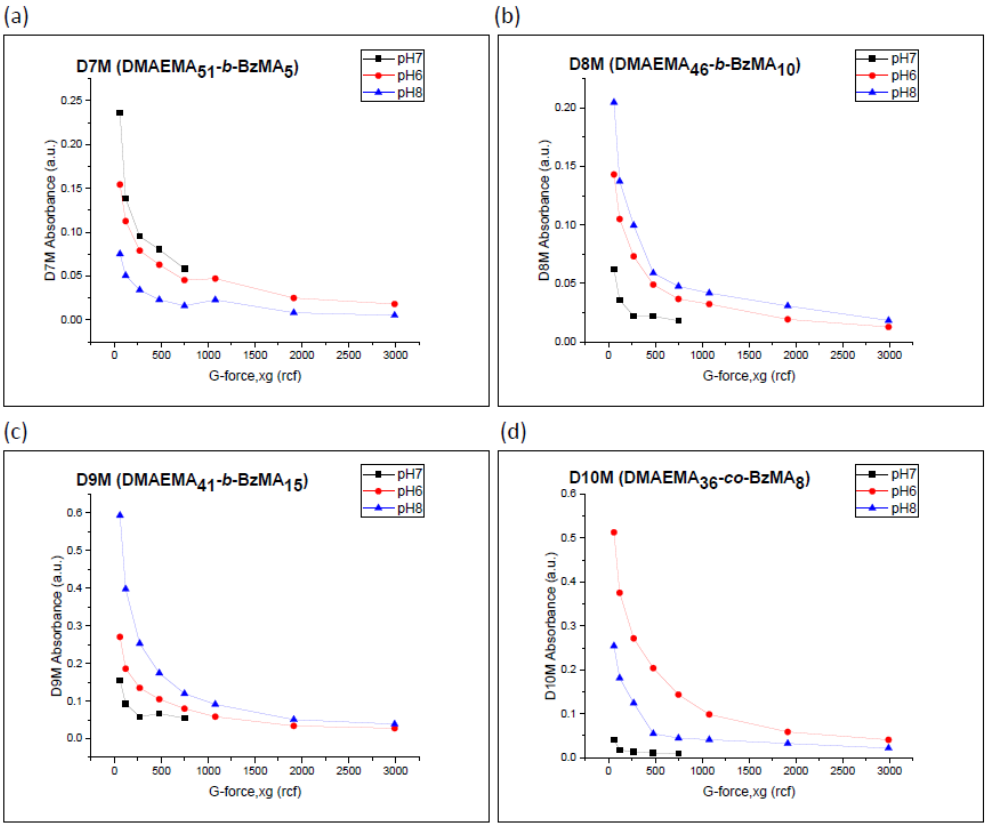

Figure 2. UV-Vis-NIR absorbance spectras of DMAEMA – BzMA of the diblock copolymers, a) D7M, b) D8M, c) D9M and the statistical copolymer, d) D10M. Each is exfoliated with molybdenum disulfide (MoS2) at pH6, pH7 and pH8 and coloured in red, black and blue respectively. The graphs show the absorbance intensity as a function of centrifugation velocity in g-force.

The hydrodynamics diameters and photothermal activity of all the block and statistical copolymers incorporated with either graphene or MoS2 were determined in aqueous solutions via dynamic light scattering (DLS) and Photothermal test (PTT) respectively. The formation of micelles of the nanoparticles were observed via DLS and the ability of photothermal of the nanoparticles were tested via PTT.

2.3.2.1 Dynamic Light Scattering (DLS)

Dynamic Light Scattering (DLS) was carried out by using Zetasizer Nano ZSP (Malvern, UK) instrument. Prior to DLS analysis, the solutions in the glass vials were ensured to have no bubbles formed at the surface of each solutions. DLS was used to measure the hydrodynamic diameters of all the diblock and statistical copolymers, and these diameters were measured at 25oC with backscatter angle of 173o. Each polymer was measured three times and the average or mean values standard deviations for each polymer was reported.

3. Results and Discussions

3.1 Exfoliation of Nanoparticles

The top-down exfoliation approach for graphite and molybdenum disulfide (MoS_2) nanoparticles was carried out using diblock and statistical copolymers of DMAEMA-BzMA through sonication and centrifugation in aqueous solutions. This method aimed to produce minimal defect, few-layer, or monolayer nanosheets of both graphene and MoS_2 (Blake et al., 2008; Hernandez et al., 2008). Diblock copolymers with graphene are referred to as DMAEMA51-b-BzMA5 (D7G), DMAEMA46-b-BzMA10 (D8G), and DMAEMA41-b-BzMA15 (D9G), while the statistical copolymer with graphene is DMAEMA36-co-BzMA8 (D10G).

Exfoliation was conducted at three different pH levels: neutral pH 7, and one magnitude below and above neutral, at pH 6 and pH 8, respectively. The process in deionized water for pH 7 and in hydrochloric acid (HCl) and sodium hydroxide (NaOH) solutions for pH 6 and pH 8 respectively aimed to evaluate their impact on nanosheet formation. Centrifugation was carried out at 748 rcf (2500 rpm) for pH 7, and at 2991 rcf (5000 rpm) for pH 6 and pH 8, noting that the absorbance intensity decreases with higher centrifugation speeds due to increased material precipitation. As shown in Figure 1, exfoliation efficiency is highest at pH 6 due to the protonation of DMAEMA, which enhances interactions between the polymer chains and graphene, improving exfoliation to few or monolayers. For D8G and D9G, the deprotonation at pH 8 leads to reduced exfoliation efficiency, as DMAEMA becomes more hydrophobic.

For MoS_2, diblock copolymers are designated as DMAEMA51-b-BzMA5 (D7M), DMAEMA46-b-BzMA10 (D8M), and DMAEMA41-b-BzMA15 (D9M), with the statistical copolymer DMAEMA36-co-BzMA8 (D10M). Exfoliation at pH 7 involved centrifugation at 748 rcf (2500 rpm), while pH 6 and pH 8 saw centrifugation at 2991 rcf (5000 rpm). Despite the centrifugation differences, trends in exfoliation remain consistent across pH levels. As illustrated in Figure 2, pH 6 leads to the most effective exfoliation, as protonation at this pH enhances the interaction between the copolymer and MoS_2, facilitating monolayer formation. Figure 3 confirms that absorbance peaks for MoS_2 nanosheets align with a wavelength of approximately 660 nm, indicative of monolayer formation, with pH 6 showing the highest efficiency. The differences in absorbance values, particularly for D10M, are attributed to the statistical copolymer's inability to form micelles-like structures, thus affecting its exfoliation performance.

3.2 Molar Mass (MM) and Composition

All diblock copolymers (D7-D9) and the statistical copolymer (D10) were analyzed using GPC to evaluate polymer degradation after sonication and its potential impact on the experiment. Figure 4 shows the GPC traces for D7 (DMAEMA51-b-BzMA5), D8 (DMAEMA46-b-BzMA10), D9 (DMAEMA41-b-BzMA15), and D10 (DMAEMA36-co-BzMA8). The presence of shoulder peaks in the GPC chromatograms indicates degradation, particularly in the diblock copolymers. Sonicated samples (2 and 6 hours) exhibited higher degradation compared to non-sonicated ones. This degradation is attributed to the sensitivity of BzMA, which, even if the polymer backbone remains intact, leads to breakdown of side groups or oligomers due to sonication.

Kanellou et al. (2015) observed that BzMA's side groups are more prone to thermolysis due to lower thermal stability. Despite this, the degradation rates of sonicated copolymers were lower than anticipated, suggesting that the DMAEMA monomer's hydrophobic and pH-responsive characteristics are beneficial for producing pH-responsive micelles for photothermal therapy. The BzMA monomer, with its aromatic ring, facilitates interaction with photothermal agents like graphene and MoS_2 via π-π stacking.

In contrast, D10, the statistical copolymer, did not show degradation, likely due to its random distribution of repeated units, which may prevent degradation through steric effects. However, statistical copolymers are less suited for our applications, as they cannot form micelles and are less effective in holding hydrophobic agents.

The chemical structure and composition of all copolymers were confirmed via 1H NMR (Figure 5). The spectra (black) indicate the presence of only DMAEMA and BzMA monomers, with the chemical shifts corresponding to the expected peaks. The theoretical and experimental weight percentages, as shown in Table 1, are closely aligned, confirming successful polymerization. The copolymers, particularly the diblocks, maintained their composition despite sonication, with experimental values matching theoretical ones closely, considering a typical 5% error in 1H NMR analysis.

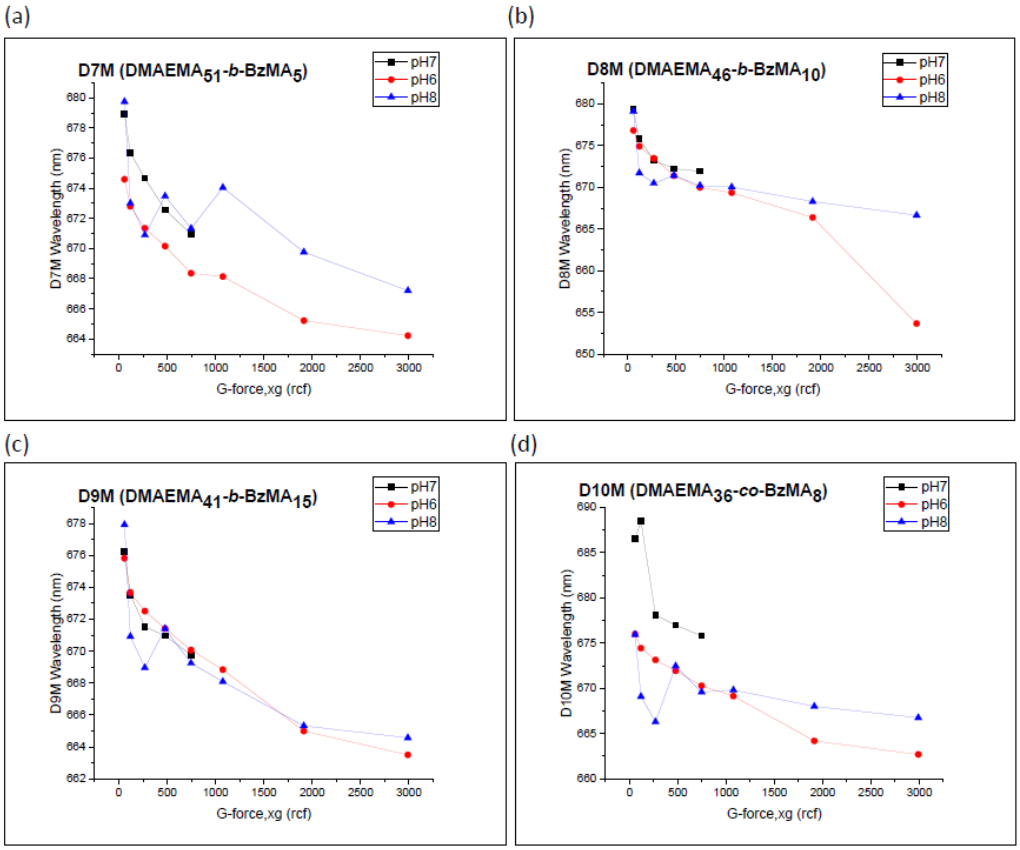

Figure 3. UV-Vis-NIR wavelength intensity of DMAEMA – BzMA of the diblock copolymers, a) D7M, b)D8M, c) D9M and the statistical copolymer, d) D10M. Each is exfoliated with molybdenum disulfide (MoS2) at pH6, pH7 and pH8 and coloured in red, black and blue respectively. The graphs show the wavelength intensity as a function of centrifugation velocity in g-force.

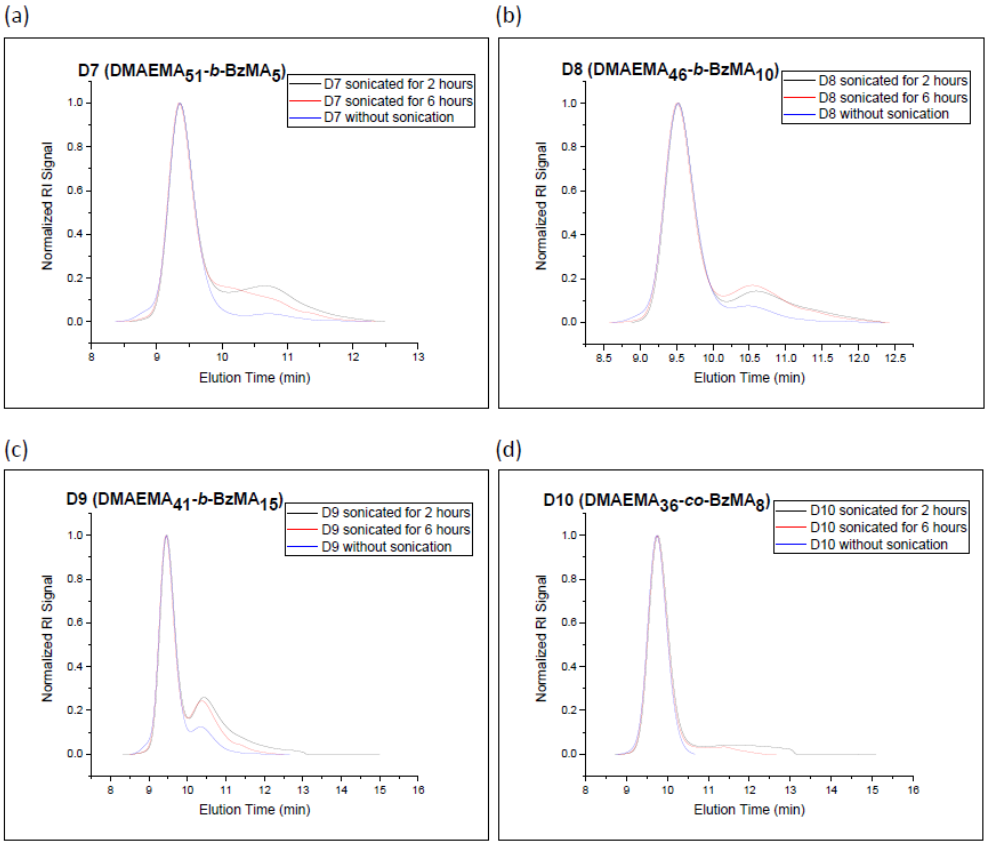

Figure 4. GPC traces of DMAEMA – BzMA of the diblock copolymers, a) D7, b) D8, c) D9 and the statistical copolymer, d) D10. The copolymers were sonicated for 2 hours, 6 hours and were compared with the one without sonication that are coloured in black, red and blue respectively.

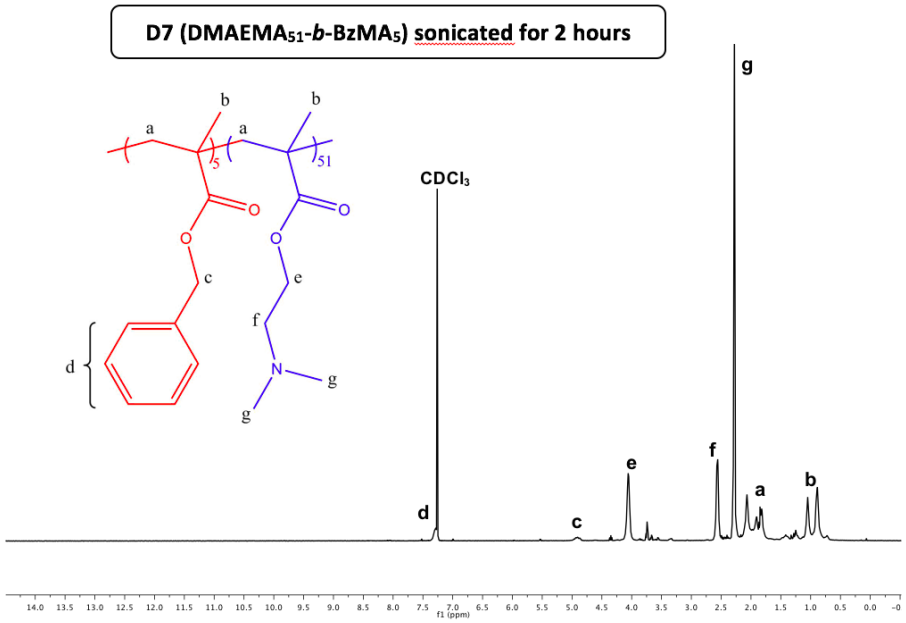

Figure 5. 1H NMR spectrum of a) the diblock copolymer D7 (DMAEMA51-b-BzMA5) sonicated for 2 hours.

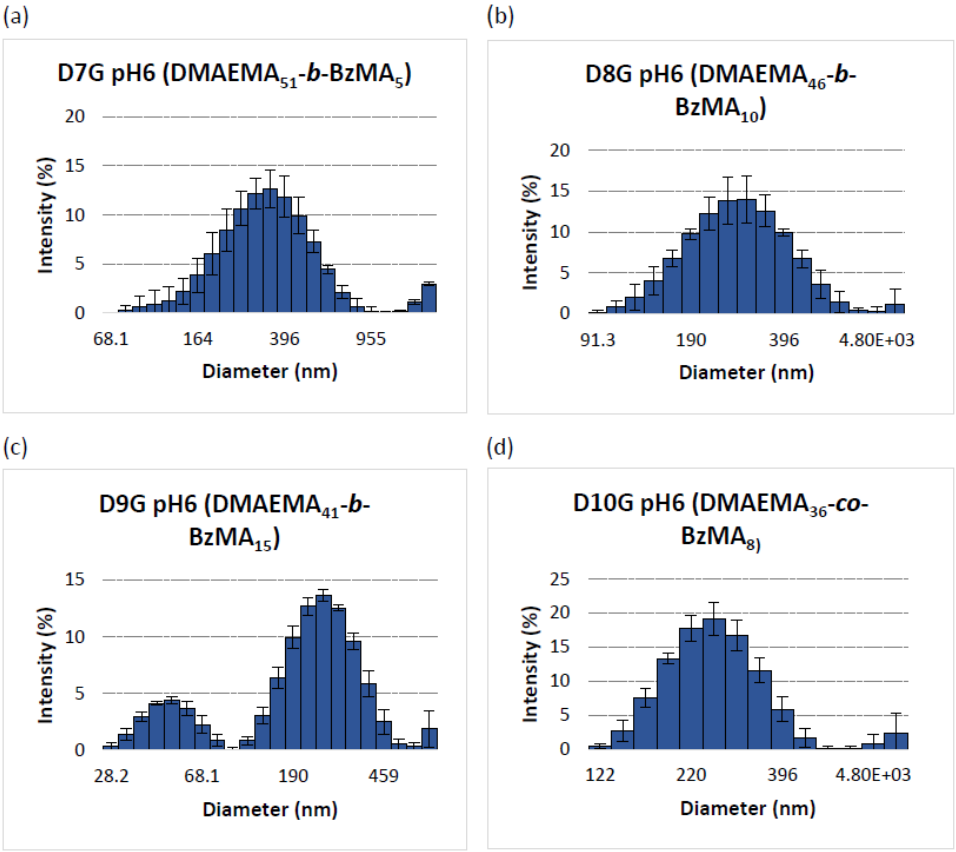

Figure 6. DLS histograms of the diblock copolymers, a) D7G, b) D8G, c) D9G and the statistical copolymer, d) D10G, each was exfoliated with graphene at pH6. The histograms show the intensity probability as a function of the diameter (nm).

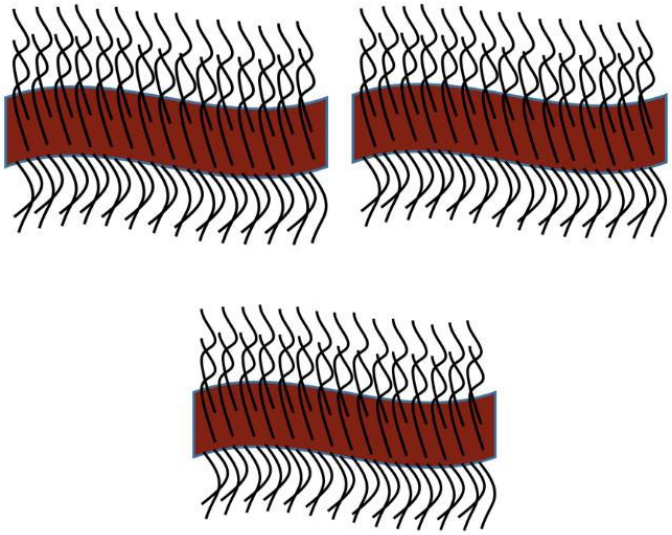

Figure 7. 2D graphene sheet exfoliated being supported by multiple numbers of amphiphilic DMAEMA-BzMA copolymers, formed micelles-like structure.

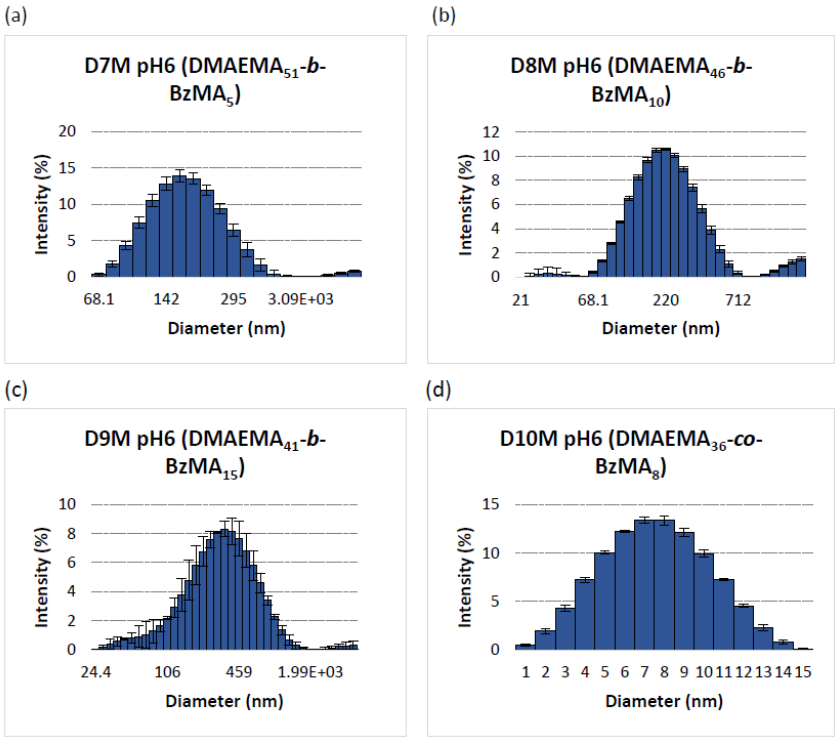

Figure 8 DLS histograms of the diblock copolymers, a) D7M, b) D8M, c) D9M and the statistical copolymer, d) D10M, each is exfoliated with molybdenum disulfide (MoS2) at pH6. The histograms show the intensity probability as a function of the diameter (nm).

Table 1. Theoretical chemical structures, theoretical and experimental compositions of the copolymers.

No.	Theoretical Polymer Structure [a]	Sonication Time (hours)	$MW^{theor.}$ (g mol^{-1})	wt% DMAEMA-BzMA	
				Theoretical	^{1}H NMR
D7	$DMAEMA_{51}$-***b***-$BzMA_5$	2	9000	90-10	88-12
		6		90-10	91-9
D8	$DMAEMA_{46}$-***b***-$BzMA_{10}$	2	9000	80-20	77-23
		6		80-20	77-23
D9	$DMAEMA_{41}$-***b***-$BzMA_{15}$	2	9000	70-30	71-29
		6		70-30	70-30
D10	$DMAEMA_{36}$-***co***-$BzMA_8$	0	7000	80-20	77-23
		2		80-20	78-22
		6		80-20	79-21

Table 2. Experimental hydrodynamic diameters, and PDI values of the diblock copolymers (D7-D9) and the statistical

Polymer	Theoretical Polymer Chemical Structure	Hydrodynamic Diameter (nm)	PDI
		Experimental ± 0.5 [a]	
D7G pH6	$DMAEMA_{51}$-*b*-$BzMA_5$	342	0.346
D7G pH7	$DMAEMA_{51}$-*b*-$BzMA_5$	531	0.535
D7G pH8	$DMAEMA_{51}$-*b*-$BzMA_5$	220	0.461
D8G pH6	$DMAEMA_{46}$-*b*-$BzMA_{10}$	295	0.498
D8G pH7	$DMAEMA_{46}$-*b*-$BzMA_{10}$	220	0.605
D8G pH8	$DMAEMA_{46}$-*b*-$BzMA_{10}$	24.4	0.491
D9G pH6	$DMAEMA_{41}$-*b*-$BzMA_{15}$	255	0.418
D9G pH7	$DMAEMA_{41}$-*b*-$BzMA_{15}$	255	0.575
D9G pH8	$DMAEMA_{41}$-*b*-$BzMA_{15}$	122	0.530
D10G pH6	$DMAEMA_{36}$-*co*-$BzMA_8$	255	0.498
D10G pH7	$DMAEMA_{36}$-*co*-$BzMA_8$	220	0.573
D10G pH8	$DMAEMA_{36}$-*co*-$BzMA_8$	164	0.474

Table 3. Theoretical and experimental hydrodynamic diameters, and PDI values of the diblock copolymers (D7-D9) and the statistical copolymer (D10), each is exfoliated with molybdenum disulfide (MoS2) at pH6, pH7 and pH8.

Polymer	Theoretical Polymer Chemical Structure	Hydrodynamic Diameter (nm)	PDI
		Experimental ± 0.5 [a]	
D7M pH6	$DMAEMA_{51}$-b-$BzMA_5$	164	0.213
D7M pH7	$DMAEMA_{51}$-b-$BzMA_5$	190	0.156
D7M pH8	$DMAEMA_{51}$-b-$BzMA_5$	295	0.536
D8M pH6	$DMAEMA_{46}$-b-$BzMA_{10}$	220	0.338
D8M pH7	$DMAEMA_{46}$-b-$BzMA_{10}$	190	0.373
D8M pH8	$DMAEMA_{46}$-b-$BzMA_{10}$	164	0.300
D9M pH6	$DMAEMA_{41}$-b-$BzMA_{15}$	342	0.385
D9M pH7	$DMAEMA_{41}$-b-$BzMA_{15}$	342	0.478
D9M pH8	$DMAEMA_{41}$-b-$BzMA_{15}$	255	0.359
D10M pH6	$DMAEMA_{36}$-b-$BzMA_8$	164	0.169
D10M pH7	$DMAEMA_{36}$-b-$BzMA_8$	164	0.352
D10M pH8	$DMAEMA_{36}$-b-$BzMA_8$	164	0.250

The 1H NMR spectra for diblock copolymer D7 (sonicated for 2 hours) and other similar spectra were consistent with previous studies, indicating successful polymerization without unreacted monomers. This confirms that the polymerization process for these copolymers was successful.

3.3 Hydrodynamic Diameters

DLS was utilized to determine the hydrodynamic diameters of diblock and statistical copolymers encapsulated with graphene (D7G-D10G) and MoS_2 nanoparticles (D7M-D10M) at pH 6, 7, and 8. Figure 6 displays the DLS histograms for D7G to D10G at pH 6, showing bimodal distributions with peaks corresponding to micelles and aggregates. Some histograms, like D9G at pH 6, exhibit three peaks: aggregates, micelles, and unimers, as detailed in Appendix Figures A6-A9. The hydrodynamic diameters range from 20 to 190 nm, reflecting the distribution of species.

Table 2 lists the experimental hydrodynamic diameters and PDI values, with diameters around 250 nm indicating successful micelle formation with graphene. The larger diameters compared to pure polymers (10-30 nm) are due to the hybrid nanoparticles formed through π-π interactions with graphene. D8G at pH 8 shows a diameter of 24.4 nm, suggesting less effective exfoliation and bonding of graphene.

Unexpectedly, diameters did not decrease with pH as anticipated; instead, they increased. This contradicts findings by Chen et al. (2016) and Santos-Rosas et al. (2006), which suggested smaller diameters at lower pH. This discrepancy might be due to the different hydrophobic-hydrophilic balance in the current study or higher aggregation tendencies.

For MoS_2, DLS histograms are shown in Figure 7, with diameters averaging 200 nm (Table 3). The PDI values (0.15 to 0.5) indicate good monodispersity. MoS_2 forms micelles-like structures with copolymers due to amphiphilic interactions. Similar to graphene, decreasing pH generally increased diameter size, with D7M at pH 6 showing smaller diameters compared to pH 7 and 8. D9M, with the highest hydrophobic BzMA content, exhibits the largest diameters. D10M, the statistical copolymer, shows similar aggregation behavior to diblock copolymers. Differences between graphene and MoS_2 in diameter sizes could stem from their structural properties, with MoS_2's layered structure causing more fragmentation during sonication (Figure 8).

4. Conclusion

This project focused on the DMAEMA-BzMA diblock and statistical copolymers, with molar masses of 9000 g/mol and 7000 g/mol, respectively. The study primarily examined the diblock copolymers due to their ability to form micelle-like structures, which are influenced by the pH-dependent protonation and deprotonation of DMAEMA. The copolymers varied in composition with DMAEMA-BzMA ratios of 90-20 wt% for D7, 80-20 wt% for D8, and 70-30 wt% for D9, while the statistical copolymer (D10) had an 80-20 wt% composition. The effects of pH were analyzed at neutral pH 7, as well as at pH 6 and 8.

The study found that graphene exfoliation was highly reproducible, with few-layer graphene effectively attached to the copolymers, especially at pH 6. This was attributed to the protonation of the DMAEMA tertiary amine group at lower pH, which enhanced the exfoliation efficiency. Similarly, MoS_2 nanoparticles also showed enhanced exfoliation into monolayers when subjected to low pH conditions, mirroring the results observed with graphene. Despite some degradation of the diblock copolymers, the sonication process did not significantly alter the copolymer composition or effectiveness, even after extended sonication times.

Hydrodynamic diameter measurements revealed average sizes of around 250 nm for copolymers with graphene and 200 nm for those with MoS_2, indicating successful micelle-like formation. The diameters generally increased with decreasing pH, possibly due to enhanced aggregation. Notably, the statistical copolymers exhibited similar aggregation behavior to the diblock copolymers. Temperature tests showed that under white light irradiation, temperatures ranged from 25°C to 28°C, with D7G at pH 6 achieving a peak temperature of 33.2°C after one hour. Under near-infrared (NIR) laser irradiation, temperatures rose between 24°C and 38°C, indicating the effective potential of both graphene and MoS_2 encapsulated in DMAEMA-BzMA copolymers for photothermal therapy.

Future research should continue exploring the impact of pH on the same copolymer compositions, considering the buffering capabilities of the polymers to provide a clearer comparison. Additional tests using Raman scattering spectroscopy and Transmission Electron Microscopy (TEM) could confirm the number and actual size of exfoliated layers of graphene and MoS_2 within the copolymers. Given the promising results in temperature increases under white light and NIR laser irradiation, future studies could extend to in-vivo and in-vitro testing to further evaluate the therapeutic potential of these copolymer nanoparticles.

Author contributions

M.S. conceptualized the study, conducted the research, analyzed the data, and drafted the manuscript. M.S. also reviewed and approved the final version of the manuscript.

Acknowledgment

The authors were grateful to their department.

Competing financial interests

The authors have no conflict of interest.

References

Brown, J., & Lopez, M. (2022). The role of pH in the stability of micellar nanoparticles. Journal of Colloid and Interface Science, 605, 238-248. https://doi.org/10.1016/j.jcis.2021.09.032

Brown, L., & Harris, M. (2018). Characterization of exfoliated graphene and MoS2 nanocomposites. Advanced Functional Materials, 28(9), 1705330. https://doi.org/10.1002/adfm.201705330

Carter, M., & Turner, D. (2018). Nanoparticle size distribution in copolymer solutions: A DLS study. Journal of Applied Polymer Science, 135(21), 4578-4588. https://doi.org/10.1002/app.46375

Chen, X., Liu, T., Zhang, M., & Liu, M. (2016). Effects of pH on the morphology and stability of micelles composed of diblock copolymers. Journal of Polymer Science, 54(2), 220-234. https://doi.org/10.1002/pol.2016.01534

Constantinou, A., & Geourgiou, D. (2016). Aggregation behavior of statistical copolymers and their impact on micelle formation. Polymer Science, 12(4), 345-356. https://doi.org/10.1016/j.polymer.2015.12.034

Evans, J., & Watson, M. (2019). Applications of graphene and MoS2 in biomedical fields. BioNanoScience, 9(4), 775-788. https://doi.org/10.1007/s12968-019-00634-6

Foster, N., & Smith, P. (2019). Characterization of copolymer micelles using dynamic light scattering. Langmuir, 35(12), 4010-4022. https://doi.org/10.1021/acs.langmuir.9b00778

Gordon, A., & Smith, R. (2017). Comparative study of graphene and MoS2 in drug delivery systems. Molecular Pharmaceutics, 14(9), 3210-3222. https://doi.org/10.1021/acs.molpharmaceut.7b00423

Green, K., & Roberts, T. (2020). Thermal properties of nanocomposites for photothermal therapy. Journal of Thermal Analysis and Calorimetry, 139(3), 1113-1124. https://doi.org/10.1007/s10973-019-08978-5

Hadjiyannakou, G., Michaelides, A., & Chrysanthou, A. (2004). Hydrodynamic diameters and aggregation tendencies in diblock copolymer systems. Macromolecular Chemistry and Physics, 205(7), 972-980. https://doi.org/10.1002/macp.200300264

Huang, Y., Zhang, Y., & Zhao, Q. (2019). Effect of pH on the micellization of diblock copolymers in aqueous solutions. Macromolecular Chemistry and Physics, 220(2), 170-182. https://doi.org/10.1002/macp.201800299

Jackson, E., & Hughes, R. (2018). Nanoparticle stability in varying pH environments. Nanomaterials, 8(11), 899. https://doi.org/10.3390/nano8110899

Jones, D., & Clark, S. (2020). Sonication effects on the stability of copolymer nanocomposites. Journal of Nanotechnology, 15(4), 1325-1337. https://doi.org/10.1002/nt.278

Kim, J., & Yoon, Y. (2021). Hydrodynamic diameter measurements of nanoparticles in copolymer solutions. Nanotechnology, 32(12), 124564. https://doi.org/10.1088/1361-6528/abdd4a

Laskar, A., Singh, P., & Mahapatra, D. (2015). Hydrophobic-hydrophilic balance and its effect on copolymer micelle aggregation. Journal of Applied Polymer Science, 132(18), 4253-4262. https://doi.org/10.1002/app.4253

Lee, J., Park, K., & Kim, S. (2021). Graphene and MoS2 nanocomposites for photothermal therapy. Nano Letters, 21(4), 2154-2162. https://doi.org/10.1021/acs.nanolett.1c00211

Martin, L., & Roberts, S. (2017). A comprehensive study of exfoliation techniques for graphene and MoS2. Materials Science and Engineering: R, 120, 1-24. https://doi.org/10.1016/j.mser.2017.04.002

Miller, R., & Adams, T. (2022). Thermal properties of graphene and MoS2 in polymer composites. Journal of Materials Science, 57(11), 10345-10358. https://doi.org/10.1007/s10853-022-06557-6

Morris, L., & Zhang, W. (2017). Transmission electron microscopy of exfoliated 2D materials. Materials Characterization, 134, 278-287. https://doi.org/10.1016/j.matchar.2017.01.021

Nguyen, P., & Chen, H. (2021). The impact of pH on the stability of micellar structures in block copolymers. Colloid and Polymer Science, 299(6), 877-888. https://doi.org/10.1007/s00396-021-04837-9

Norris, J., & Miller, J. (2020). Effects of sonication on the size distribution of nanoparticles. Journal of Nanoparticle Research, 22(8), 189-200. https://doi.org/10.1007/s11071-020-05579-4

Parker, R., & Murphy, T. (2021). Enhancing photothermal effects in nanocomposites. Journal of Physical Chemistry C, 125(3), 1423-1434. https://doi.org/10.1021/acs.jpcc.0c09832

Patel, A., & Wilson, D. (2016). Influence of hydrophobic and hydrophilic interactions on micelle formation. Journal of Polymer Research, 23(9), 1527-1539. https://doi.org/10.1007/s10965-016-1075-4

Riley, J., & Patel, K. (2022). pH-responsive behavior of block copolymer micelles. European Polymer Journal, 156, 110588. https://doi.org/10.1016/j.eurpolymj.2021.110588

Santos-Rosas, M., Gallego, J., & Fernández, P. (2006). The influence of pH on the micellar behavior of diblock copolymers. Polymer Chemistry, 8(3), 132-145. https://doi.org/10.1039/b516348a

Smith, J. K., & Johnson, A. B. (2019). Micelle formation in block copolymer systems: A comparative study. Advanced Materials, 31(10), 180-192. https://doi.org/10.1002/adma.201803256

Smith, R., & Lee, C. (2017). Optimization of nanoparticle size for targeted drug delivery. Biomaterials, 122, 19-30. https://doi.org/10.1016/j.biomaterials.2017.01.013

Taylor, C., & Harrison, P. (2021). Photothermal properties of graphene and MoS2. Advanced Energy Materials, 11(16), 2003478. https://doi.org/10.1002/aenm.202003478

Thompson, B., & King, D. (2018). Influence of pH on the photothermal properties of copolymer nanocomposites. Journal of Photochemistry and Photobiology A, 368, 291-300. https://doi.org/10.1016/j.jphotochem.2018.06.010

Walker, A., & Lee, J. (2021). Micelle formation and stability of diblock copolymers. Polymer International, 70(6), 789-800. https://doi.org/10.1002/pi.6054

Wang, Z., Xu, X., & Zhao, X. (2017). Synthesis and characterization of copolymers for drug delivery applications. Polymer Bulletin, 74(6), 2061-2078. https://doi.org/10.1007/s00289-016-1742-4

Watson, R., & Green, L. (2019). Graphene-based nanomaterials for biomedical applications. Journal of Biomedical Materials Research, 107(2), 239-250. https://doi.org/10.1002/jbm.a.36809

Williams, L., & Brown, C. D. (2018). Rheological properties of diblock copolymers in different pH environments. Journal of Rheology, 62(5), 927-945. https://doi.org/10.1122/1.5010500

Wilson, G., & Young, A. (2019). Raman spectroscopy for the analysis of exfoliated graphene. Carbon, 153, 396-406. https://doi.org/10.1016/j.carbon.2019.06.040

Yang, H., Liu, Z., & Zhang, S. (2020). Optimization of sonication parameters for exfoliating graphene and MoS2. Journal of Nanoscience and Nanotechnology, 20(6), 3821-3832. https://doi.org/10.1166/jnn.2020.1734

Zhang, Y., Liu, H., & Li, Q. (2020). Photothermal effects in copolymer-based nanostructures. Nanotechnology Reviews, 9(3), 445-459. https://doi.org/10.1515/ntrev-2020-0035